OCCAM

OXFORD CENTRE FOR COLLABORATIVE APPLIED MATHEMATICS

Mathematical Biomedicine and Modeling Avascular Tumor Growth

by

Helen M. Byrne

OCCAM Preprint Number 12/96

12

Mathematical Biomedicine and Modeling Avascular Tumor Growth

Helen M. Byrne

12.1 Continuum Models of Avascular Tumor Growth

Abstract. In this chapter we review existing continuum models of avascular tumor growth, explaining how they are inter-related and the biophysical insight that they provide. The models range in complexity and include one-dimensional studies of radially-symmetric growth, and two-dimensional models of tumor invasion in which the tumor is assumed to comprise a single population of cells. We also present more detailed, multiphase models that allow for tumor heterogeneity. The chapter concludes with a summary of the different continuum approaches and a discussion of the theoretical challenges that lie ahead.

Keywords. Avascular Tumor Growth, Cancer, Hypoxia, Mathematical Modeling, Moving Boundary Problem, Multicellular Tumor Spheroid, Multiphase Model, Partial Differential Equation

2010 Mathematics Subject Classification. 35Q92, 92B05

12.1.1 Introduction

Cancer is a complex, multi-factorial disease which continues to devastate lives and cause widespread morbidity and mortality throughout the world. The vast amounts of money that have been invested in cancer research have undoubtedly advanced understanding of how the disease progresses and contributed to the significant increases in five-year survival rates for certain types of cancer, including breast and colon. Unfortunately this trend does not apply to all cancers, with survival rates for brain tumors and cervical cancer showing little change since 1985. Further, it has been argued that the increases in survival rates should be attributed to better screening programs and earlier diagnosis rather than scientific advances.

While debates about the societal benefit of cancer research will continue to excite interest for years to come, it is less controversial to view cancer as a multistage disease, characterized by the progressive loss of function of a range of regulatory genes, including repair genes that correct mutations and DNA damage before cell division and tumor suppressor genes that signal for cell-cycle arrest or induce programmed

* This publication was based on work supported in part by Award No. KUK-C1-013-03, made by King Abdullah University of Science and Technology (KAUST).

cell death (apoptosis) if substantial genetic damage is detected [53]. The uncontrolled division of a mutated cell leads to the growth of a (small) avascular tumor, which will then remain dormant unless it is eliminated by immune surveillance or it acquires its own blood system by the process of angiogenesis. The resulting vascular tumor is well supplied with nutrients and may increase rapidly in size. Finally, malignant tumors are able to invade the surrounding tissue, leading to metastatic spread, with secondary tumors arising elsewhere in the host. Further genetic mutations within the tumor mass may endow it with drug resistance and facilitate its later stages of development.

The complex pattern of vascular tumor growth, combined with the paucity of reliable experimental assays for collecting dynamic data from the same tumor, have deterred many theoreticians from attempting to model this phase of tumor growth [9, 79, 99]. Fortunately, the situation is starting to change, stimulated in large part by technological advances which make it possible now simultaneously to visualize changes in the size and spatial composition of vascular tumors using certain experimental assays. Thus, as we look to the future, we should anticipate the development of realistic models of vascular tumor growth that have been validated against experimental data. However, it will be some years before this vision becomes a reality and there are assays for vascular tumor growth which generate data which are as accurate and reproducible as those obtained when clusters of tumor cells are cultured *in vitro* as multicellular spheroids [67]. For these reasons, in this chapter we will focus on reviewing theoretical efforts to describe the early phase of avascular tumor growth.

During avascular growth, externally-supplied nutrients are consumed by live, proliferating cells as they diffuse toward the tumor center. As the tumor grows, the amount of nutrient reaching the center declines until there is insufficient to sustain viable cells. There ensues the formation of a central core of dead (necrotic) cellular material whose size increases as the tumor continues to grow. Thus, a well-developed avascular tumor comprises an outer rim of nutrient-rich, proliferating cells and a central core of nutrient-starved, necrotic debris. These regions may be separated by a layer of oxygen-poor (hypoxic) cells which are quiescent (viable but nonproliferating). Since diffusion controls the delivery of nutrients (e.g., oxygen and glucose) to, and the removal of waste products from, avascular tumors [38, 95], the diameter to which they may grow is typically limited to several millimetres, growth halting when the rate of volume increase of the tumor balances its rate of volume loss, increases being due to cell growth and proliferation and decreases to cell death.

There is a large theoretical literature devoted to mathematical models of the growth of avascular tumors and multicellular tumor spheroids. While in this chapter attention will focus on deterministic models that can be formulated as mixed systems of partial differential equations (PDEs), we pause here to mention some of the other approaches that are being used. These include discrete, cell-based models which view the tumor as a collection of interacting cells, each assigned their own set of parameter values and behavioral rules [6, 92]. Such models are gaining in popularity and have been used to study not only the growth of multicellular tumor spheroids [61, 71] but

also tumor invasion [34, 103] and the fixation of clonal sub-populations within the intestinal crypt [104]. Additionally, Anderson and coworkers have used cellular automata models to investigate how the microenvironment (specifically, the local oxygen concentration and extracellular matrix density) influences (and is influenced by) the growth dynamics and phenotypic diversity of a tumor [7, 86]. Their simulations predict that when oxygen levels are low the tumor will rapidly diverge from its initial phenotype and exhibit high levels of population diversity, with aggressive phenotypes quickly becoming dominant.

In this chapter we present a series of increasingly complex, spatially-structured models of avascular growth, starting in Section 12.1.2 with one-dimensional models. The stability of these models to symmetry-breaking perturbations is considered in Section 12.1.3 and the results used to determine conditions under which a radially-symmetric tumor remains compact and localized (i.e., stability) and conditions under which it is predicted to become irregularly shaped and invasive (i.e., instability). In Section 12.1.4 we use a multiphase modeling framework to extend the models from Sections 12.1.2 and 12.1.3 to allow for tumor heterogeneity. In so doing, we not only provide justification for the use of Darcy's law to describe cell motion (this law states that cells move down pressure gradients) but also enable other descriptions of the tumor's material properties to be incorporated. The chapter concludes in Section 12.1.5 with a summary of the models presented and a discussion of future theoretical challenges.

12.1.2 Diffusion-limited Models of Avascular Tumor Growth

12.1.2.1 Introduction

In this section we consider the earliest continuum models for multicellular tumor spheroids growing in free suspension [11, 49, 90]. We view the tumor as a radially-symmetric and spatially-uniform mass of cells whose net growth rate is determined by local levels of a single, diffusible species (such as oxygen or glucose) which is present in the culture medium that surrounds the spheroids. As we explain below, these models couple a reaction-diffusion equation for the growth-rate limiting nutrient $c(r,t)$ to an integro-differential equation for the outer tumor radius $R(t)$, with additional equations defining implicitly internal boundaries $R_H(t)$ and $R_N(t)$ that mark the transitions between nutrient-rich regions of cell proliferation, and nutrient-poor regions of hypoxia and necrosis. The governing equations are introduced in Subsection 12.1.2.2 and analyzed in Subsection 12.1.2.3. We identify conditions under which the models reduce to a nonlinear ordinary differential equation for $R(t)$ and algebraic equations for the internal free boundaries, $R_H(t)$ and $R_N(t)$. The section concludes in Subsection 12.1.2.4 with a summary of the biological insights that these models, and their extensions, can provide and a discussion of their shortcomings.

12.1.2.2 Model Development

In order to describe the radially-symmetric growth of an avascular cluster of tumor cells growing in free suspension, we introduce dependent variables $R(t)$ and $c(r,t)$ to represent respectively the size of the tumor radius at time $t > 0$ and the concentration of a single, growth-rate limiting, diffusible chemical (henceforth oxygen) at time t and distance r from the cluster center ($0 \leq r \leq R(t)$). We denote by $r = R_H(t)$ and $r = R_N(t)$ the internal boundaries that mark the transitions between regions of cell proliferation, quiescence and necrosis. The principle of mass balance is used to derive equations for $c(r,t)$ and $R(t)$, whereas $R_H(t)$ and $R_N(t)$ are defined implicitly, occurring when the oxygen concentration $c(r,t)$ passes through known threshold values.

The Oxygen Concentration, $c(r,t)$. We assume that the dominant processes regulating the distribution of oxygen within the spheroid are diffusive transport and its consumption by the tumor cells. Combining these processes we deduce that $c(r,t)$ satisfies the following reaction-diffusion equation:

$$\frac{\partial c}{\partial t} = \underbrace{\frac{D}{r^2}\frac{\partial}{\partial r}\left(r^2\frac{\partial c}{\partial r}\right)}_{\substack{\text{diffusive}\\ \text{transport}}} - \underbrace{\Gamma(c, R, R_H, R_N)}_{\substack{\text{rate of oxygen}\\ \text{consumption}}}, \tag{12.1}$$

where D denotes the assumed constant diffusion coefficient of the oxygen and $\Gamma = \Gamma(c)$ its rate of consumption. In practice, $\Gamma(c)$ will be a non-linear function which depends on the tumor cell line under investigation. Here, for simplicity and to demonstrate the qualitative behavior of the model, we suppose that oxygen is consumed at the constant rate Γ by both proliferating and quiescent cells and so we fix

$$\Gamma(c) = \Gamma H(c - c_N),$$

where $H(.)$ denotes the Heaviside step function ($H(x) = 1$ if $x > 0$ and $H(x) = 0$ otherwise) and c_N denotes the threshold oxygen concentration at which cells become necrotic (i.e., live cells are restricted to regions where $c > c_N$).

The Outer Tumor Radius, $R(t)$. We assume that the oxygen distribution determines $S(c)$ and $N(c)$, the local rates of cell proliferation and cell death at all points within the tumor, and use the principle of mass balance to derive the following equation for the evolution of the outer tumor radius, $R(t)$:

$$\underbrace{\frac{d}{dt}\left(\frac{4\pi R^3}{3}\right)}_{\substack{\text{rate of change}\\ \text{of tumor volume}}} = \underbrace{\iiint S(c)\, r^2 \sin\theta \; d\theta \; d\varphi \; dr}_{\substack{\text{total rate}\\ \text{of cell proliferation}}} - \underbrace{\iiint N(c)\, r^2 \sin\theta \; d\theta \; d\varphi \; dr}_{\substack{\text{total rate}\\ \text{of cell death}}},$$

where, for radially-symmetric growth, $c = c(r,t)$ and the above equation reduces to

$$R^2 \frac{dR}{dt} = \int_0^{R(t)} [S(c) - N(c)]\, r^2\, dr. \tag{12.2}$$

As simple, representative examples, we assume that cell proliferation is localized in nutrient-rich regions (where $c > c_H$) where it occurs at a rate which is proportional to the local nutrient concentration, c. We suppose further that both apoptosis (or natural cell death) and necrosis contribute to cell death, with apoptosis occurring at a constant rate throughout the tumor and necrosis being localized to nutrient-starved regions (where $c \leq c_N < c_H$). Thus, we fix

$$S(c) = scH(c - c_H) \quad \text{and} \quad N(c) = s\lambda_A + s\lambda_N H(c_N - c),$$

where s, λ_A and λ_N are positive constants.

The Hypoxic and Necrotic Boundaries, $R_H(t)$ and $R_N(t)$. The internal free boundaries $r = R_H(t)$ and r=$R_N(t)$ are defined implicitly in terms of threshold oxygen concentrations c_H and $c_N < c_H$. These constants denote respectively the minimum oxygen concentration at which cell proliferation can occur and the minimum concentration at which quiescent cells can remain alive. Three different cases arise according to whether the minimum oxygen concentration within the tumor falls below none, one or both these threshold values:

- **Case 1:** uniformly proliferating tumor ($R_N(t) = R_H(t) = 0$). In this case, $c(r,t) > c_H \ \forall\ r \in (0, R(t))$.
- **Case 2:** central quiescent core surrounded by a proliferating annulus ($R_N(t) = 0 < R_H(t) < R(t)$). In this case, $c(r,t) > c_N \ \forall\ r \in (0, R)$ so that $R_N(t) = 0$ and there exists $0 < R_H(t) < R(t)$ such that $c(r,t) \leq c_H$ for $r \in (0, R_H)$, $c_H < c(r,t)$ for $r \in (R_H, R)$ and
$$c(R_H, t) = c_H.$$
- **Case 3:** fully-developed spheroid ($0 < R_N(t) < R_H(t) < R(t)$). In this case,
$$c(R_N, t) = c_N \text{ and } c(R_H, t) = c_H.$$
with $c(r,t) \leq c_N$ for $r \in (0, R_N)$, $c_N < c(r,t) < c_H$ for $r \in (R_N, R_H)$ and $c(r,t) > c_H$ for $r \in (R_H, R)$.

We consider each of these cases in turn in Subsection 12.1.2.3. In Figure 12.1 we provide a schematic diagram to illustrate the structure of a well-developed avascular tumor which possesses a central necrotic core and a hypoxic region.

Our model comprises equations (12.1)–(12.2) for $c(r,t)$ and $R(t)$ and supplementary equations for $R_H(t)$ and $R_N(t)$. It remains to specify appropriate boundary and

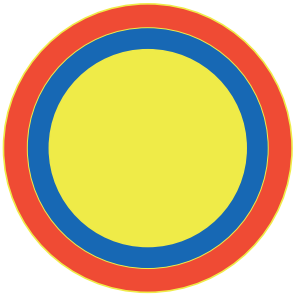

Figure 12.1. Schematic diagram of a fully-developed avascular tumor. An outer proliferating rim (the red region, where $c > c_H$ and $R_H \leq r \leq R$) surrounds a hypoxic or quiescent annulus (the blue region, where $c_N < c < c_H$ and $R_N \leq r \leq R_H$) and a central necrotic core (the yellow region, where $c(r,t) \leq c_N$ and $o \leq r \leq R_N$).

initial conditions to close the model. We assume symmetry of the oxygen profile about $r = 0$, that on the outer tumor boundary it is maintained at a constant value, $c = c_\infty$ say. Finally, we prescribe the initial tumor radius ($R(0) = R_0$) and the initial oxygen distribution ($c(r,0) = c_0(r)$). Thus we have

$$\left.\begin{aligned} \frac{\partial c}{\partial r} &= 0 \qquad \text{at } r = 0, \\ c &= c_\infty \quad \text{on } r = R(t), \\ c,\ \frac{\partial c}{\partial r} &\text{ continuous across } r = R_H(t) \text{ and } r = R_N(t), \\ c(r,0) &= c_0(r),\ R(t=0) = R_0. \end{aligned}\right\} \tag{12.3}$$

Nondimensionalization. Before analyzing the model equations, we recast them in dimensionless variables. Denoting typical length and time scales by X and T and a typical oxygen concentration by C, we introduce the following dimensionless variables

$$r^* = \frac{r}{X}, \quad t^* = \frac{t}{T}, \quad c^* = \frac{c}{C}, \quad R^* = \frac{R}{X}, \quad R_H^* = \frac{R_H}{X}, \quad R_N = \frac{R_N}{X}.$$

When written in terms of dimensionless variables, our model equations become

$$\frac{\partial c^*}{\partial t^*} = \left(\frac{DT}{X^2}\right)\frac{1}{r^{*2}}\frac{\partial}{\partial r^*}\left(r^{*2}\frac{\partial c^*}{\partial r^*}\right) - \Gamma T H(c^* - c_N^*),$$

$$R^{*2}\frac{dR^*}{dt^*} = \int_0^{R^*} \left\{sTCc^*H(c^* - c_N^*) - \lambda_A^* - \lambda_N^* H(c_N^* - c^*)\right\} r^{*2}\, dr^*.$$

where $\lambda_A^* = sT\lambda_A$ and $\lambda_N^* = sT\lambda_N$. Guided by our interest in timescales on which the tumor's size and spatial structure change, we focus on the tumor doubling timescale and choose

$$T = \frac{1}{sC}.$$

Following [49], we exploit the fact that the oxygen diffusion timescale ($\sim$ minutes) is much shorter than a typical tumor doubling time ($\sim$ weeks or months) and make a quasi-steady approximation in the nutrient equation so that

$$0 = \frac{1}{r^{*2}}\frac{\partial}{\partial r^*}\left(r^{*2}\frac{\partial c^*}{\partial r^*}\right) - \Gamma^* H(c^* - c_N^*),$$

where $\Gamma^* = \frac{\Gamma X^2}{D} \sim O(1)$ (we remark that, as a result, prescription of the initial oxygen profile in (12.3) is redundant).

For completeness, we now state our dimensionless model equations in full, omitting the $*$s for clarity:

$$0 = \frac{1}{r^2}\frac{\partial}{\partial r}\left(r^2\frac{\partial c}{\partial r}\right) - \Gamma H(c - c_N), \tag{12.4}$$

$$R^2\frac{dR}{dt} = \int_0^R \{cH(c - c_N) - \lambda_A - \lambda_N H(c_N - c)\}\, r^2 dr, \tag{12.5}$$

$$R_H = 0 \text{ if } c > c_H \ \forall\ r \text{ and otherwise } c(R_H, t) = c_H, \tag{12.6}$$

$$R_N = 0 \text{ if } c > c_N \ \forall\ r \text{ and otherwise } c(R_N, t) = c_N, \tag{12.7}$$

$$\frac{\partial c}{\partial r} = 0 \quad \text{at } r = 0, \tag{12.8}$$

$$c = c_\infty \quad \text{on } r = R, \tag{12.9}$$

$$R(0) = R_0, \text{ prescribed.} \tag{12.10}$$

We remark that c_∞ could be eliminated from the model equations by fixing $C = c_\infty$. We want to investigate the effect of varying c_∞ and, hence, retain it as an explicit model parameter. For similar reasons, we choose not to scale lengths with R_0.

12.1.2.3 Model Analysis

In this subsection we derive analytical expressions for $c(r, t)$ and show how the model may be reduced to a nonlinear ordinary differential equation (ODE) for $R(t)$ and algebraic equations for $R_H(t)$ and $R_N(t)$. We show further how the form of these relations changes as $R(t)$ increases, and we progress from Case 1 to Cases 2 and 3.

Case 1: Uniformly Proliferating Tumor. In this case, $R_H = R_N = 0$ and equations (12.4)–(12.10) reduce to give

$$c(r,t) = c_\infty - \frac{\Gamma}{6}(R^2 - r^2),$$
$$\frac{dR}{dt} = \frac{R}{3}\left(c_\infty - \frac{\Gamma R^2}{15} - \lambda_A\right), \tag{12.11}$$

where, for valid solutions, $c(r,t) > c_H$ for $0 < r < R(t)$. This growth phase persists until either the tumor attains a steady state (at which $\frac{dR}{dt} = 0$) or the model ceases to be valid.

Recalling that a spherically-symmetric tumor of radius $R(t)$ has volume $V(t) = 4\pi R^3(t)/3$, we remark that equation (12.11) is equivalent to

$$\frac{1}{V}\frac{dV}{dt} = c_\infty - \lambda_A - \frac{\Gamma}{15}\left(\frac{3V}{4\pi}\right)^{2/3}.$$

Thus, our spatially-structured model for the growth of a uniformly proliferating avascular tumor exhibits the same dynamics as a time-dependent, ODE. However, without performing the above analysis, it would not be obvious what powers of V to include or how to relate the model parameters to physically defined quantities.

From (12.11) we deduce that $\frac{dR}{dt} = 0$ when $R = 0$ (the trivial solution) or, assuming $c_\infty > \lambda_A$, when $R = [15(c_\infty - \lambda_A)/\Gamma)]^{1/2}$. Linear stability analysis reveals that the trivial solution is unstable if $c_\infty > \lambda_A$ (i.e., where a nontrivial steady state exists) and stable otherwise.

As stated above, the nontrivial steady state is physically realistic if $c(r,t) > c_H \; \forall \, r \in (0, R)$. Since c attains a minimum at $r = 0$ we deduce that $R = [15(c_\infty - \lambda_A)/\Gamma)]^{1/2}$ is a physically realistic steady state if

$$c_\infty < 5\lambda_A - 2c_H.$$

In practice, λ_A and c_H will be fixed for a given tumor cell line. If $\lambda_A < 2c_H/5$ then the above inequality never holds, irrespective of c_∞, and no non-trivial steady state solution exists. By contrast, if $\lambda_A > 2c_H/5$ then we predict that for $\lambda_A < c_\infty < 5\lambda_A - 2c_H$, there is a nontrivial steady state with $0 = R_H = R_N < R$ and which linear stability analysis shows to be stable. For $c_\infty > 5\lambda_A - 2c_H$, the model breaks down before the steady state is attained, a region of quiescence forming when $R = [6(c_\infty - c_H)/\Gamma]^{1/2}$.

Case 2: Intermediate-sized Tumor. In this case $R_N = 0$ and equations (12.4)–(12.10) supply

$$c(r,t) = c_\infty - \frac{\Gamma}{6}(R^2 - r^2),$$
$$\frac{dR}{dt} = \frac{R}{3}\left[\left(c_\infty - \frac{\Gamma R^2}{6}\right)\left(1 - \frac{R_H^3}{R^3}\right) + \frac{\Gamma R^2}{10}\left(1 - \frac{R_H^5}{R^5}\right) - \lambda_A\right], \tag{12.12}$$

where

$$R_H^2 = R^2 - \frac{6}{\Gamma}(c_\infty - c_H), \tag{12.13}$$

and for valid solutions $c(r,t) > c_N$ for $0 < r < R(t)$.

By differentiating (12.13) with respect to time, we can recast our model as a pair of ODEs for R and R_H, with

$$\frac{dR_H}{dt} = \frac{R}{R_H}\frac{dR}{dt}.$$

Since $0 < R_H < R$, we deduce that $|\frac{dR_H}{dt}| > |\frac{dR}{dt}|$. Thus, if the tumor contains a quiescent region, then $R_H(t)$ changes more rapidly than $R(t)$. In particular, it the tumor is growing (i.e., $\frac{dR}{dt} > 0$) then the quiescent region is growing more rapidly. We remark that, instead of differentiating (12.13) with respect to time we could use it to eliminate R_H from (12.12) and, in so doing, reduce the model to a single, nonlinear ODE for $R(t)$. In contrast to equation (12.11), the resulting ODE does not lend itself to physical interpretation. In this case, the absence of a clear link between the spatially-structured model and the corresponding ODE model underlines the difficulty associated with relating the parameters that appear in spatially-homogeneous models to physically relevant quantities.

As for Case 1, by setting $d/dt = 0$ in equation (12.12), it is possible to identify conditions under which the system evolves to a nontrivial steady state. This equilibrium solution is physically realistic provided that $c_N < c_{min} = c_\infty - \Gamma R^2/6 > c_H$ or, equivalently, $6(c_\infty - c_H)/\Gamma < R^2 < 6(c_\infty - c_N)/\Gamma$. Otherwise, assuming $dR/dt > 0$, so that the tumor is increasing in size, a central necrotic core will form and we must consider Case 3.

Case 3: Fully-developed Tumor. In this case $0 < R_N(t) < R_H(t) < R(t)$ and the model equations reduce to give

$$c(r,t) = \begin{cases} c_N & 0 < r < R_N, \\ c_N + \Gamma(r - R_N)^2(r + 2R_N)/6r & R_N < r < R, \end{cases} \tag{12.14}$$

$$\frac{dR}{dt} = \frac{R}{3}\left[c_N\left(1 - \frac{R_H^3}{R^3}\right) - \left(\lambda_A + \lambda_N\frac{R_N^3}{R^3}\right)\right] + \frac{\Gamma R^3}{6}\left[\frac{1}{5}\left(1 - \frac{R_H^5}{R^5}\right) - \frac{R_N^2}{R^2}\left(1 - \frac{R_H^3}{R^3}\right) + \frac{R_N^3}{R^3}\left(1 - \frac{R_H^2}{R^2}\right)\right], \tag{12.15}$$

with

$$\left(1 - \frac{R_N}{R}\right)^2\left(1 + \frac{2R_N}{R}\right) = \frac{6}{\Gamma R^2}(c_\infty - c_N), \tag{12.16}$$

and

$$\left(1 - \frac{R_N}{R_H}\right)^2\left(1 + \frac{2R_N}{R_H}\right) = \frac{6}{\Gamma R_H^2}(c_H - c_N). \tag{12.17}$$

Once again, the model reduces to a nonlinear ODE for $R(t)$. However, in this case the ODE is coupled to two algebraic equations for R_H and R_N. While it is, in principle, possible to use equations (12.16) and (12.17) to eliminate both R_H and R_N from (12.15), the complexity of the resulting ODE means that it is more informative to consider equations (12.15)–(12.17) together.

12.1.2.4 Discussion

In this section we have studied simple, radially-symmetric models of avascular tumor growth and shown how the governing equations can be used to determine how the size and structure of the tumor change over time and how the long-time or equilibrium composition of the tumor depend on physical parameters such as c_∞, the concentration of a diffusible nutrient such as oxygen which is supplied externally, and λ_A, the basal level of cell death due to apoptosis.

We remark that the kinetic terms used in our analyses are highly idealized and should be replaced by functions which have been fitted to experimental data [87]. In general, these functions will be non-linear and the resulting models must be solved numerically. Whilst numerical simulations are of great value, they may obscure the manner in which the various mechanisms interact. In such cases, complementary insight into the system's dynamics can be gained by using asymptotic techniques to study cases for which the model equations simplify greatly. For example, in [21], when the tumor is small (so that $0 < R \ll 1$ and $R_H = R_N = 0$), equation (12.11) predicts exponential growth of $R(t)$. Alternatively, if $c_\infty - c_N \ll 1$ and $\lambda_A + \lambda_N \ll 1$ then, since $c_N < c_H < c_\infty$, we deduce that $c_\infty - c_H \ll 1$ while equations (12.15)–(12.17) imply that the tumor will evolve to a non-trivial equilibrium, with a thin proliferating rim ($0 < R - R_H \ll 1$) and a thin quiescent rim ($0 < R - R_N \ll 1$). This resembles the structure of MCS cultured *in vitro* where, typically, the outer viable rim is only three to seven cell layers thick [38].

There are many ways in which the model presented above has been extended. In addition to using experimentally-determined functions for the rates of cell proliferation, apoptosis and necrosis, additional reaction-diffusion equations can be incorporated to describe the action of other diffusible growth factors which may be present in the tumor environment. These chemicals may be supplied externally or expressed by the tumor cells themselves and may promote or inhibit the tumor's growth. For example, bi-products of the degradation process that accompany cellular necrosis are believed to inhibit cell proliferation (models of this type are studied in [20, 49]). If we view the nutrient as a (growth-) activator and the bi-product of necrosis as an inhibitor, it may be possible to apply classical Turing theory to this reaction-diffusion system in order to determine whether the system will generate spatial patterns, with hot-spots of high cell density [26]. Similarly, it is possible to include a more realistic description of cell metabolism by introducing separate variables to describe oxygen, glucose, pH and lactate. In models that distinguish between normal and tumor cells, this enables

us to investigate the advantage over normal cells that tumor cells enjoy under acidosis [47, 91, 108]. Alternatively, the models can be used to investigate the response of tumors to treatment with radiotherapy and/or chemotherapy [37, 58, 60].

A further model extension which provides a simple description of vascular tumor growth involves including a distributed source of nutrient (or a distributed sink of waste products) in the outer portion of the tumor so that, in place of equation (12.4), we use

$$0 = \frac{1}{r^2}\frac{\partial}{\partial r}\left(r^2\frac{\partial c}{\partial r}\right) + h(c_{\text{vess}} - c)H(c - c_H) - \Gamma H(c - c_N),$$

where h and c_{vess} denote respectively the rate at which oxygen exchanges with the vasculature and the oxygen concentration within the vessels. As a result, nutrients may be supplied to the tumor either by exchange with its vasculature or by diffusion across the tumor's outer boundary (for details, see [18, 19]).

The models presented in this section can be termed moving boundary problems since the domain on which they are formulated (i.e., the tumor size) must be determined as part of the solution procedure. As such, they have excited the interest of Friedman and coworkers who have constructed proofs of existence and uniqueness of the model solutions [29, 32, 45], that place the earlier analysis on a more rigorous footing.

Given that avascular tumors are usually radially-symmetric while vascular tumors possess highly irregular boundaries, it is natural to ask whether this change in morphology is due to the non-uniform distribution of blood vessels vascularization or whether the radially-symmetric avascular tumors are intrinsically unstable to asymmetric perturbations. Although the spatially-structured models presented in this section are not amenable to such analysis, in the next section we show how they have been extended to address this important question.

12.1.3 Tumor Invasion

12.1.3.1 Introduction

In this section we show how the one-dimensional models of Section 12.1.2 have been extended to study avascular tumor growth in two and three dimensions, following an approach originally proposed by Greenspan [50] in which new dependent variables for the local cell velocity and pressure within the tumor were introduced. The physical principles that underpin models of this type can be summarized as follows: if the tumor is incompressible and contains no voids or holes, then cell proliferation and death generate spatial variations in the pressure within the tumor which drive cell motion, with cells moving down pressure gradients, away from regions of net cell proliferation and toward regions of net cell death. Surface tension is also incorporated into the model as a mechanism for maintaining the tumor's compactness and counteracting the expansive force caused by cell proliferation.

The remainder of this section is organized as follows. In Subsections 12.1.3.2 and 12.1.3.3 we develop the model equations and show how the models of Section 12.1.2 are recovered when growth is one-dimensional. The stability of steady, radially-symmetric solutions to symmetry-breaking perturbations is investigated in Subsection 12.1.3.4 before the section concludes, in Subsection 12.1.3.5, with a discussion of the models and suggestions for further research.

12.1.3.2 The Model Equations

The model that we study is presented below in dimensionless form (for details, see [20, 50]). For simplicity, we assume that the tumor is small enough that it is nutrient-rich, with all cells proliferating and, hence, that there is no quiescence or necrosis. The key variables are the nutrient concentration $c(\boldsymbol{r}, t)$, the cell velocity $\boldsymbol{v}(\boldsymbol{r}, t)$ and the pressure $p(\boldsymbol{r}, t)$. The variables c, $\boldsymbol{v}$ and p satisfy the following system of dimensionless partial differential equations

$$0 = \nabla^2 c - \Gamma, \tag{12.18}$$

$$\nabla \cdot \boldsymbol{v} = S(c) - N(c) \equiv c - \lambda_A, \tag{12.19}$$

$$\boldsymbol{v} = -\mu \nabla p. \tag{12.20}$$

Equation (12.18) is the natural extension in higher spatial dimensions of the quasi-steady reaction-diffusion equation that was used in Section 12.1.2. Equation (12.19) expresses mass conservation within the (assumed incompressible) tumor. We highlight similarities with the models from Section 12.1.2 by employing the same proliferation and death rates here. Following [50], in equation (12.19) Darcy's law relates the cell velocity to the pressure, with cells moving down pressure gradients and the constant of proportionality μ denoting the sensitivity of the tumor cells to the pressure gradients.

Equations (12.19) and (12.20) can be combined to eliminate $\boldsymbol{v}$ from the model equations, giving

$$0 = \mu \nabla^2 p + (c - \lambda_A). \tag{12.21}$$

Equations (12.18) and (12.21) are closed by imposing the following boundary conditions:

$$\frac{\partial c}{\partial r} = \frac{\partial p}{\partial r} = 0 \quad \text{at} \quad \boldsymbol{r} = 0. \tag{12.22}$$

$$c = c_\infty, \quad p = \gamma \kappa \quad \text{on} \quad \Gamma(\boldsymbol{r}, t) = 0, \tag{12.23}$$

Equations (12.22) guarantee that the nutrient and pressure profiles are bounded at the origin. In (12.23), c_∞ and $p_\infty = 0$ are the assumed constant nutrient concentration and pressure outside the tumor, $\gamma \geq 0$ is the surface tension coefficient and κ the mean curvature of the tumor boundary, on which $\Gamma(\boldsymbol{r}, t) = 0$. Thus, equations (12.23) state that the nutrient concentration is continuous across the tumor boundary and that there is a jump discontinuity in the pressure, this jump being proportional to the curvature

of the boundary (and playing the role of a surface tension force which maintains the tumor's compactness).

In order to complete our model, it remains to determine how the tumor boundary $\Gamma(\boldsymbol{r}, t) = 0$ evolves. Following [50], we write $\boldsymbol{r} = (r, \theta)$ and parameterize the tumor boundary as follows

$$\Gamma(\boldsymbol{r}, t) = 0 = r - R(\theta, t).$$

We assume further that cells located on the boundary move with the local velocity there so that

$$\frac{\partial R}{\partial t} = \boldsymbol{v} \cdot \boldsymbol{n}|_{r=R(\theta,t)} = -\mu \nabla p \cdot \boldsymbol{n}|_{r=R(\theta,t)}, \tag{12.24}$$

with $R(\theta, t = 0) = R_0(\theta)$.

In Equation (12.24), $\boldsymbol{n}$ is the unit outward normal to the tumor boundary and $R_0(\theta) = r$ denotes the position of the tumor boundary at $t = 0$.

In summary, our model of solid tumor growth comprises equations (12.18) and (12.21)–(12.24).

12.1.3.3 Radially-Symmetric Model Solutions

Under the assumption of radial symmetry, $c = c(r, t)$, $p = p(r, t)$, $r = R(t)$ on the tumor boundary and the model equations reduce to give

$$0 = \frac{1}{r^2}\frac{\partial}{\partial r}\left(r^2 \frac{\partial c}{\partial r}\right) - \Gamma, \tag{12.25}$$

$$0 = \frac{\mu}{r^2}\frac{\partial}{\partial r}\left(r^2 \frac{\partial p}{\partial r}\right) + (c - \lambda_A), \tag{12.26}$$

$$\frac{dR}{dt} = -\mu \frac{\partial p}{\partial r}\bigg|_{r=R(t)}. \tag{12.27}$$

Integrating equation (12.26) once with respect to r and imposing (12.22), we deduce that

$$-\mu \frac{\partial p}{\partial r} = \frac{1}{r^2}\int_0^r (c - \lambda_A)\rho^2 d\rho \;\Rightarrow R^2 \frac{dR}{dt} = \int_0^R (c - \lambda_A) r^2 dr, \tag{12.28}$$

which shows how the current model reduces to the simpler models presented in Section 12.1.2 under radial symmetry.

By integrating equations (12.25)–(12.26) subject to the boundary conditions, we obtain the following expressions for c and p:

$$c(r, t) = c_\infty - \frac{\Gamma}{6}(R^2 - r^2),$$

$$p(r, t) = \frac{\gamma}{R} - \frac{\Gamma}{120\mu}(R^2 - r^2)^2 + \frac{1}{6\mu}\left(c_\infty - \lambda_A - \frac{\Gamma R^2}{15}\right)(R^2 - r^2).$$

Substitution with $c(r,t)$ in (12.28) then yields

$$\frac{dR}{dt} = \frac{R}{3}\left(c_\infty - \lambda_A - \frac{\Gamma R^2}{15}\right),$$

which is identical to equation (12.11), showing how the current model reduces to Case 1 from Section 12.1.2 under the assumption of radial symmetry.

12.1.3.4 Linear Stability Analysis

In this subsection, we investigate what happens when steady radially-symmetric solutions are subjected to small, symmetry-breaking perturbations. Our aim is to identify conditions under which the perturbations grow over time and conditions under which they decay: in the former case the radially-symmetric solution is said to be unstable (to symmetry-breaking perturbations) and in the latter it is stable. For simplicity, we consider the stability of steady radially-symmetric solutions by seeking solutions to the governing equations of the form

$$\left.\begin{array}{rcl} c & \sim & c_0(r) + \epsilon c_1(r,\theta,t) \\ p & \sim & p_0(r) + \epsilon p_1(r,\theta,t) \\ R & \sim & R_0 + \epsilon R_1(\theta,t) \end{array}\right\} \quad \text{where } 0 < \epsilon \ll 1. \tag{12.29}$$

and, from Section 12.1.3.3,

$$c_0(r) = c_\infty - \frac{\Gamma}{6}(R_0^2 - r^2), \quad p_0(r) = \frac{\gamma}{R_0} - \frac{s\Gamma}{120\mu}(R_0^2 - r^2)^2,$$

and

$$R_0^2 = \frac{15}{\Gamma}(c_\infty - \lambda_A). \tag{12.30}$$

Substituting with (12.29) in equations (12.18), (12.21), (12.24), (12.23) and (12.22) and equating to zero coefficients of $O(\epsilon)$ we deduce that (c_1, p_1, R_1) solve

$$0 = \nabla^2 c_1 = \nabla^2 p_1 + c_1, \tag{12.31}$$

$$\frac{\partial R_1}{\partial t} = -\mu\left[\frac{\partial p_1}{\partial r} + R_1 \frac{d^2 p_0}{dr^2}\right]_{r=R_0}, \tag{12.32}$$

with

$$\frac{\partial c_1}{\partial r} = \frac{\partial p_1}{\partial r} = 0 \quad \text{at } r = 0, \tag{12.33}$$

$$c_1 = -R_1 \left.\frac{dc_0}{dr}\right|_{r=R_0}, \tag{12.34}$$

$$p_1 = -R_1 \left.\frac{dp_0}{dr}\right|_{r=R_0} - \frac{\gamma}{R_0^2}\left(2R_1 + \mathcal{L}(R_1)\right)_{r=R_0}, \tag{12.35}$$

$$R_1(\theta,0) = R_{10}(\theta), \quad \text{prescribed.} \tag{12.36}$$

In (12.35),

$$\mathcal{L}(f) = \frac{1}{\sin\theta}\frac{\partial}{\partial\theta}\left(\sin\theta\frac{\partial f}{\partial\theta}\right)$$

so that

$$\nabla^2 f(r,\theta) = \frac{1}{r^2}\frac{\partial}{\partial r}\left(r^2\frac{\partial f}{\partial r}\right) + \frac{\mathcal{L}(f)}{r^2}.$$

We remark that the derivation of equation (12.35) involves determining the $O(\epsilon)$ contributions to the curvature and the normal derivative of the pressure on the tumor boundary (details of these calculations are contained in references [20, 49]).

Equations (12.31)–(12.36) are linear and, hence, admit separable solutions of the form

$$\left.\begin{aligned} c_1(r,\theta,t) &= \chi_k(t) r^k P_k(\cos\theta) \\ p_1(r,\theta,t) &= \left(\pi_k(t) - \frac{\chi_k r^2}{2\mu(2k+3)}\right) r^k P_k(\cos\theta) \\ R_1(\theta,t) &= \rho_k(t) P_k(\cos\theta) \end{aligned}\right\} \tag{12.37}$$

where the Legendre polynomials $P_k(\cos\theta)$ satisfy $\mathcal{L}(P_k) = -k(k+1)P_k$ so that $\nabla^2(r^k P_k) = 0$. It is straightforward to show that equations (12.31) and (12.33) are automatically satisfied by the above choice of c_1 and p_1.

The coefficients χ_k and π_k are determined by imposing conditions (12.35) and exploiting the orthogonality of the Legendre polynomials. This gives

$$\chi_k R_0^k = -\frac{\Gamma R_0}{3}\rho_k \quad \text{and} \quad \pi_k R_0^k = \frac{\gamma\rho_k}{2R_0^2}(k-1)(k+2) + \frac{\chi_k R_0^{k+2}}{2\mu(2k+3)}.$$

Using these results in (12.32) we deduce that the amplitude ρ_k of a perturbation to the tumor radius, $R(\theta,t)$, involving $P_k(\cos\theta)$ satisfies

$$\frac{1}{\rho_k}\frac{d\rho_k}{dt} = (k-1)\left(\frac{2\Gamma R_0^2}{15(2k+3)} - \frac{\gamma\mu}{2R_0^3}k(k+2)\right). \tag{12.38}$$

From (12.38) we note that all modes evolve independently and that the system is insensitive to perturbations involving the first Legendre polynomial (the latter result is unsurprising since $P_{k=1}(\cos\theta)$ corresponds simply to a translation of the co-ordinate axes). We note also that if surface tension effects are neglected ($\gamma = 0$) then the radially-symmetric steady state is unstable to all modes for which $k \geq 2$. More generally, if $\gamma > 0$ then the steady state is unstable to the finite number of modes for which

$$k(k+2)(2k+3) < \frac{4\Gamma R_0^5}{15\mu\gamma}.$$

Since the steady state radius R_0 is defined in terms of the system parameters (see equation (12.30)), this result shows how the choice of parameter values influences

the modes to which the steady state is unstable. We note also that as γ increases, the number of unstable modes falls. In particular, if $2\Gamma R_0^5/15\mu\gamma < 15$ then there are no integers which satisfy the above inequality and we deduce that in this case the radially-symmetric steady state is stable to perturbations involving Legendre polynomials of arbitrary order. Appealing to (12.30), we deduce that this will be the case if the external nutrient concentration c_∞ satisfies

$$c_\infty < \lambda + \frac{\Gamma}{15}\left(\frac{225\mu\gamma}{4\Gamma}\right)^{2/5}.$$

By differentiating (12.38) with respect to k we may determine the fastest growing mode for a given set of parameter values (and, hence, for a given value of R_0). After some manipulation, we deduce that the fastest growing mode satisfies

$$(2k+3)^2(3k^2+2k-2) = \frac{4\Gamma R_0^5}{3\mu\gamma}.$$

12.1.3.5 Discussion

The analysis presented above provides a mechanism which may explain how the irregular morphology that characterizes invasive tumors may be initiated. To understand this, consider a uniform cluster of tumor cells for which the surface tension coefficient γ is sufficiently large that the underlying radially-symmetric solution is (linearly) stable to symmetry-breaking perturbations involving Legendre polynomials. Our analysis predicts that such a cluster will remain radially symmetric throughout its development. Suppose, now, that the cells undergo a transformation which weakens the surface tension forces holding the tumor cells together. If the reduction in γ is large enough, then the tumor will become unstable to a finite range of asymmetric perturbations and develop an irregular morphology. We note that similar qualitative behavior is obtained if, instead of invoking surface tension (and the associated jump in the pressure across the tumor boundary), we assume that the nutrient concentration is discontinuous across the tumor boundary, with a jump that is proportional to the local curvature [12]. The physical motivation for this boundary condition is that nutrient (or its energy-equivalent) is utilized by cells on the tumor boundary to maintain its compactness.

Many model modifications to the basic model of asymmetric tumor growth presented in this section have been considered. These include an investigation of more general perturbations involving spherical harmonics $Y_{km}(\theta,\varphi)$, Cartesian rather than spherical geometries and a study of the stability of avascular tumors that contain quiescent and necrotic regions [13,20]. We note also that linear stability analysis predicts only local behavior. Where instability is predicted it is natural to ask how the asymmetry develops at longer times. Two complementary approaches have been used to investigate this issue. The first involves using weakly nonlinear analysis to extend the linear theory [13,24]. Alternatively, numerical methods can be used to solve the nonlinear governing equations [31].

As mentioned in Section 12.1.2, another natural extension involves incorporating additional diffusible species into the model and studying their combined effect on the tumor's development [26]. These growth factors may promote cell proliferation (e.g., oxygen and glucose) or inhibit it (e.g., tumor necrosis factor, anti-cancer drugs); they may be supplied externally (e.g., oxygen, drugs) or be produced as a bi-product of the cells' normal functions (e.g., tumor necrosis factor is a bi-product of cell degradation). Further, the introduction of cell pressure into the model makes it possible to investigate the potential influence of pressure on cell proliferation, increasing amounts of experimental data suggesting that mechanical effects have a significant influence on cell proliferation [56]. In [22], analysis of a modified version of Greenspan's basic model of asymmetric growth [50] reveals that contact-inhibition of cell proliferation (where cell proliferation halts when the cell pressure exceeds a threshold value) produces tumors whose growth dynamics are identical to those undergoing nutrient-limited growth.

Two aspects of the tumor growth model studied in this section that warrant further consideration are the assumption that the tumor cell population is spatially uniform and the use of Darcy's law to describe cell motion. In the next section we explain how a multiphase modeling approach can be used to relax these assumptions.

12.1.4 Multiphase Models of Avascular Tumor Growth

12.1.4.1 Introduction

The spatially-structured models studied thus far treat the tumor as a homogeneous mass of cells, whose proliferation and death rates are regulated by a single, diffusible species. Additionally, where it is considered, cell movement is assumed to be governed by Darcy's law, an empirical constitutive law more usually associated with fluid flow through a porous medium! Several authors have developed spatially-structured models of avascular tumor growth that account for cellular heterogeneity. For example, in [105–107] Ward and King distinguish between live and dead cells but assume that all species move with a common velocity and show how the two cell types separate to reproduce the layered structure that characterizes multicellular spheroids cultured *in vitro*. An alternative approach is employed by Thompson and Byrne [100], and Pettet and coworkers [81]: they allow for differential movement of distinct cell species but prescribe the velocities in a phenomenological manner. In this section we explain how a multiphase framework can be used to develop new models that account for cellular heterogeneity and permit the incorporation of alternative descriptions of cell movement. The models also allow for more detailed investigation of the impact that mechanical stimuli may have on cell proliferation and cell movement.

The earliest multiphase models of solid tumor growth were developed by Please and coworkers [66, 82] and based on an analogy between the layered structure of multicellular spheroids (MCS) and a compacting porous medium such as soil, the idea being that cells in the periphery are in direct physical contact (i.e., compacted) and therefore transmit any external mechanical forces that are acting whereas those in the

necrotic core are no longer in contact (they are fluidized) and so any load is distributed between the cells and the fluid. In this section we follow an alternative approach developed by Byrne and coworkers [10, 23, 25] which is based on continuum models originally developed to study the response of cartilage to mechanical loading [72]. A key difference between the multiphase models presented here and those used to study cartilage deformation is that in the latter case cell proliferation is neglected whereas in our tumor models cell proliferation (and death) must be included, leading to mass conversion between the constituent phases.

The remainder of the section is organized as follows. In Section 12.1.4.2 we develop a two-phase model of avascular tumor growth *in vitro*, the two phases representing the tumor cells and the extracellular fluid in which they are bathed. In Section 12.1.4.3 we explain how the model equations can be reduced to a simpler system of PDEs and demonstrate how the constitutive assumptions that are used to close the model influence the structure of the reduced model. For example, if the cell and fluid phases are assumed to be incompressible, with fixed volume fractions, then we recover moving boundary problems of the type presented in Section 12.1.2. Alternatively, if the two phases are treated as isotropic fluids whose pressures are related by a prescribed function of the cell volume fraction, then we recover a reaction-diffusion model of tumor invasion similar to those proposed in [46,89]. Section 12.1.4.3 also contains numerical and analytical results. We conclude in Section 12.1.4.4 by explaining how the multiphase modeling framework has been adapted to describe other aspects of solid tumor growth and outlining ideas for future work.

12.1.4.2 Model Development

Following [10, 23, 25], we view the tumor as a two-phase mixture of cells and extracellular fluid or water. For simplicity, the model is formulated in one-dimensional Cartesian geometry. We denote by $n(x,t)$ and $w(x,t)$ the volume fractions occupied by the tumor cells and extracellular fluid and by (v_n, σ_n, p_n) and (v_w, σ_w, p_w) their respective velocities, stress tensors and pressures. We derive the governing equations by applying the principles of mass and momentum balances to each phase and close the model by making constitutive assumptions about their material properties, interactions between the two phases and the factors that regulate cell proliferation and death.

The Mass and Momentum Balance Equations. Applying the principle of mass balance to n and w yields

$$\frac{\partial n}{\partial t} + \frac{\partial}{\partial x}(v_n n) = S_n, \tag{12.39}$$

$$\frac{\partial w}{\partial t} + \frac{\partial}{\partial x}(v_w w) = S_w \equiv -S_n. \tag{12.40}$$

In (12.39) and (12.40), S_n and S_w are the net rates at which cells and water are produced and we have assumed that there are no internal sources or sinks of mass so that mass is converted from one phase to the other (*i.e* $S_n = -S_w$).

Applying the principle of momentum balance to n and w, and neglecting inertial effects, we have

$$0 = \frac{\partial}{\partial x}(n\sigma_n) + F_{nw} + p\frac{\partial n}{\partial x}, \tag{12.41}$$

$$0 = \frac{\partial}{\partial x}(w\sigma_w) - F_{nw} + p\frac{\partial w}{\partial x}. \tag{12.42}$$

In (12.41) the first term represents internal forces in each phase while F_{nw} denotes the force exerted by the water on the cells, with an equal and opposite force acting on the water. The third term models interfacial effects and introduces the interfacial pressure, p. This term arises when we average over discrete cells to obtain a continuum limit (for details, see [35]). We determine p by assuming that there are no holes or voids within the tumor so that

$$n + w = 1. \tag{12.43}$$

Constitutive Assumptions. To close our model we must impose boundary and initial conditions, specify functional forms for S_n, σ_n, σ_w and F_{nw}. We start by considering the cell proliferation rate S_n that appears in (12.39). Following [25], we assume that $S_n = S_n(n, c)$ where $c(x, t)$ denotes an externally-supplied nutrient and

$$S_n(n, c) = \begin{cases} \dfrac{S_0(c - c_N)n}{1 + S_1 c} - \delta n, & \text{if } c \geq c_N, \\ -\left(\dfrac{1 + S_2\tilde{c}}{1 + S_2 c}\right) n & \text{if } c \leq c_N, \end{cases} . \tag{12.44}$$

where $S_0, S_1, S_2, c_N, \tilde{c}$ and μ are positive constants. The first term models cell proliferation as an increasing, saturating function of nutrient concentration (in practice, there is a physical limit to how rapidly cells can divide), the second models apoptosis and the third necrosis. As in earlier sections, we assume that $c(x, t)$ satisfies a quasi-steady reaction-diffusion equation and introduce positive constants Q_0 and Q_1 such that

$$0 = \frac{\partial^2 c}{\partial x^2} - \frac{Q_0 cn}{1 + Q_1 c}. \tag{12.45}$$

We remark that other choices for S_n could be used to investigate, for example, the influence on the rates of cell proliferation and death of mechanical stimuli such as pressure and shear. Theoretical studies showing how such mechanical stimuli may alter the composition of a biological tissue are presented in [75–77].

We assume that the interaction force F_{nw} is due to relative motion of the two phases and accordingly specify

$$F_{nw} = knw(v_w - v_n), \tag{12.46}$$

assuming, for simplicity, that the drag coefficient is proportional to the volume fractions of each phase, with constant of proportionality k (for other choices, see [39]).

When prescribing the stress tensors, σ_n and σ_w, we view the water as an inviscid fluid and the cell phase as a viscous fluid, with viscosity μ_n so that

$$\sigma_w = -p_w, \quad \text{and} \quad \sigma_n = -p_n + 2\mu_n \frac{\partial v_n}{\partial x}. \tag{12.47}$$

We interpret the viscosity μ_n heuristically as a measure of the cells' affinity for each other: as the cells become more pathological, and less well differentiated, they will be less likely to maintain contact with each other and/or to shear and so their viscosity will decrease.

With σ_n, σ_w and F_{nw} specified via equations (12.46)–(12.47), equations (12.41)–(12.42) define v_n and v_w. However, two additional equations are needed to determine the phase pressures p_w and p_n. For simplicity (and consistency with existing multiphase models), we fix

$$p_w = p, \tag{12.48}$$

and focus on two alternative closures for p_n. In the first case, we assume that the cell phase is incompressible so that

$$n = n^*, \tag{12.49}$$

for some positive constant $n^* \in (0, 1)$. We remark that in this case, the no-voids assumption, equation (12.43), guarantees incompressibility of the fluid phase. In the second case, we follow [25], viewing the cells as bags of water, with an additional pressure, $\Sigma(n)$ to account for the way in which cells differ from water. In more detail,

$$p_n = p + \Sigma_n(n), \tag{12.50}$$

where

$$\Sigma(n) = \begin{cases} 0 & 0 \le n < n_0, \\ \alpha \dfrac{(n - n_0)(n - n_2)}{(1 - n)^\beta} & n_0 \le n < 1, \end{cases}, \tag{12.51}$$

and

$$\beta = \frac{(1 - n_1)(3n_1 - 2n_2 - n_0)}{(n_1 - n_0)(n_2 - n_1)}, \quad \alpha = -\frac{\Sigma_1 (1 - n_1)^\beta}{(n_1 - n_0)^2 (n_2 - n_1)}.$$

Thus, if $n < n_0$ the cells exert no influence on each other. By contrast, when $n_0 < n < n_2$ the cells are attracted to each other. Finally, when $n_2 < n < 1$ the cells repel each other, the repulsive force becoming infinite as $n \to 1$. We illustrate these effects in Figure 12.2 where we sketch $\Sigma(n)$.

It remains to specify the tumor's growth rate. As in Section 12.1.3, we assume that the tumor boundary $x = R(t)$ moves with the local cell velocity there so that

$$\frac{dR}{dt} = v_n(R, t). \tag{12.52}$$

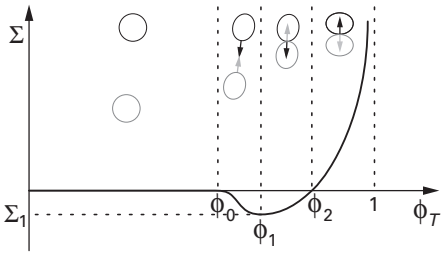

Figure 12.2. Schematic diagram showing how the function $\Sigma(n)$ varies with n. The black arrows represent the forces experienced by the black cells due to the presence of the grey cells (and conversely).

Boundary and Initial Conditions. Our two-phase model of avascular tumor growth comprises equations (12.39)–(12.52) which we close by specifying the following boundary and initial conditions:

$$v_n = 0 = v_w = \frac{\partial c}{\partial x} \quad \text{at } x = 0, \tag{12.53}$$

$$\sigma_w = -p = 0,\ \sigma_n = -p_n + 2\mu_n \frac{\partial v_n}{\partial x} = 0,\ c = c_\infty \quad \text{at } x = R(t), \tag{12.54}$$

$$n(x,0) = n_0(x),\ w(x,0) = 1 - n(x,0) = 1 - n_0(x),\ R(0) = R_0. \tag{12.55}$$

Equations (12.53) ensure symmetry about $x = 0$ while the first two of equations (12.54) guarantee continuity of (the normal component of) the cell and water stress tensors across $x = R(t)$, with the pressure outside the tumor normalized so that $p = 0$ there. Additionally, we assume that c is continuous across $x = R$ and denote by c_∞ the nutrient concentration in the surrounding medium. Finally, equations (12.55) specify the initial cell and water distributions within the tumor and its initial size.

12.1.4.3 Model Reduction

Using the constitutive assumptions specified above, it is straightforward to show that the governing equations can be written

$$\frac{\partial n}{\partial t} + \frac{\partial}{\partial x}(n v_n) = S_n, \quad \frac{\partial}{\partial x}(n v_n + (1-n) v_w) = 0, \tag{12.56}$$

$$\frac{\partial}{\partial x}\left(- n p_n - w p + 2\mu_n n \frac{\partial v_n}{\partial x} \right) = 0, \quad -\frac{\partial p}{\partial x} = k n (v_w - v_n), \tag{12.57}$$

$$0 = \frac{\partial^2 c}{\partial x^2} - \frac{Q_0 c n}{1 + Q_1 c}, \tag{12.58}$$

$$\frac{dR}{dt} = v_n(R,t), \tag{12.59}$$

wherein p_n is determined by imposing either (12.49) or (12.50).

Integrating the second of equations (12.56) subject to (12.53) and substituting in equations (12.57), we deduce that

$$v_w = -\frac{1}{k}\frac{\partial p}{\partial x},\ v_n = -\frac{w}{n}v_w = \frac{w}{kn}\frac{\partial p}{\partial x}$$

and

$$p_n = -\frac{w}{n}p + 2\mu_n\frac{\partial v_n}{\partial x} = -\frac{w}{n}p + 2\mu_n\frac{\partial}{\partial x}\left(\frac{w}{kn}\frac{\partial p}{\partial x}\right).$$

Under closure 1, $n = n^*$ and $w = 1 - n^*$ and our model simplifies further to give

$$\begin{aligned}&\frac{\partial v_n}{\partial x} = \frac{S_n}{x}\\ \Rightarrow &\frac{dR}{dt} = v_n|_{x=R(t)} = \frac{1}{n^*}\int_0^R S_n dx.\end{aligned} \tag{12.60}$$

With $S_n = S_n(n^*, c)$, the model comprises a reaction-diffusion equation for c (see equation (12.58)) and an integro-differential equation for R (see equation (12.60)), along with the appropriate boundary and initial conditions. This reduced model is equivalent to the PDE models discussed in Section 12.1.2. The analysis presented here shows how these early models of diffusion-limited growth can be viewed as special cases of the two-phase models under the assumption of incompressibility. We remark further that it is possible to relax the assumption that cell proliferation and death are dominated by the availability of diffusible nutrients and to consider, instead, situations in which these processes are regulated by mechanical phenomena. Indeed, with $S_n = S_n(p_n, p_w, v_n)$, we obtain new models whose investigation will be the subject of future work.

Under closure 2, $p_n = p + \Sigma(n)$ and our model reduces to the first of equations (12.56), together with equations (12.58), (12.59) and

$$\frac{\partial}{\partial x}\left(\mu_n n\frac{\partial v_n}{\partial x} - n\Sigma\right) = \frac{kn}{1-n}\,v_n. \tag{12.61}$$

These equations for n, v_n, c and R are solved subject to conditions (12.53)–(12.55). A typical numerical simulation taken from [25] is presented in Figure 12.3. It shows how the cell volume fraction $n(x,t) \equiv \varphi(x,t)$ and tumor radius $R(t) = L(t)$ evolve over time toward a steady state. For further details of numerical simulations and model analysis, see [10, 25].

Under the additional assumption that viscous effects are negligible, so that $\mu_n \to 0$, equation (12.61) may be used to eliminate v_n from the first of equations (12.56), yielding

$$\frac{\partial n}{\partial t} = \frac{\partial}{\partial x}\left(\frac{1-n}{k}\,\frac{\partial}{\partial x}(n\Sigma)\right) + S_n.$$

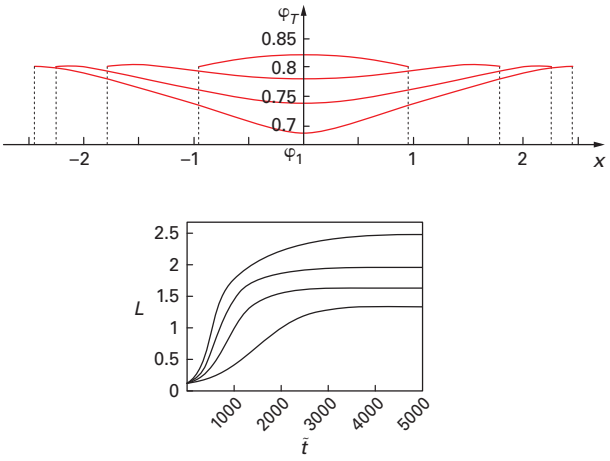

Figure 12.3. (a) Diagram showing the evolution of the cell volume fraction $n(x,t) = \varphi_T(x,t)$ toward a steady state at times $t = 500, 1\,000, 2\,000, 4\,000$; (b) Diagram showing how the evolution of the tumor radius, $R(t) = L(t)$, to its equilibrium value varies as the maximum tumor cell proliferation rate is increased. As S_0 increases, the tumor's equilibrium size increases while the time taken to reach the steady state decreases. From the lower to the upper curve S_0 increases from $S_0 = 0.005$ to $S_0 = 0.0125$.

Thus, when $\mu_n \to 0$ our model comprises a quasi-steady diffusion equation for $c(x,t)$, a nonlinear diffusion equation for n and associated boundary and initial conditions. This model is similar to existing reaction-diffusion models of tumor growth [46, 89]. The key differences here are our formulation of the problem on a moving domain and the physical mechanisms driving cell diffusion: here they are drag and cell-cell interactions rather than random cellular motion.

It is also possible to show that when viscous effects are neglected the pressures and velocities in each phase are such that

$$v_w = -\frac{1}{k}\frac{\partial p_w}{\partial x} \quad \text{and} \quad v_n = -\frac{(1-n)}{kn}\frac{\partial}{\partial x}\left(\frac{n}{1-n}p_n\right).$$

Thus for one-dimensional growth, a Darcy-type law governs the velocities of each phase, providing justification for the models of tumor growth that were originally developed by Greenspan [50] and discussed in Section 12.1.3.

12.1.4.4 Discussion

In this section we have used a multiphase approach to develop models of avascular tumor growth that account for cellular heterogeneity and permit a more general description of cell movement than was possible using the models of Sections 12.1.2 and

12.1.3. We have also shown how reaction-diffusion models can be recovered when appropriate asymptotic limits are taken and provided stronger justification for the use of Darcy's law to describe cell movement in existing phenomenological models [50].

There are many ways in which this two-phase model could be extended. Motivated by experimental work which suggests that mechanical effects can influence cell proliferation, in [25] Byrne and Preziosi assumed $S_n = S_n(c, p)$ in equation (12.44) and showed that a proliferation rate that was a decreasing function of the pressure p could limit cell growth as an alternative to nutrient limitation. A different approach was adopted in [28]. There the growth of a two-phase tumor embedded in a poroelastic gel was studied, the gel compressing in response to the expansive force exerted on it by the growing tumor mass, and exerting an equal and opposite restraining force on the tumor. The model reproduced experimental results which showed that the equilibrium size attained by a tumor spheroid cultured in such a gel decreases as the stiffness of the gel increases [56]. Roose et al. obtained similar results using a similar approach in which the tumor was treated as a two-phase poroelastic solid [88].

Other authors have developed multiphase models involving three or more phases to describe vascular tumor growth in one- and two-dimensions [9, 57], the response of tumors to treatment involving macrophages that have been genetically engineered to release anti-tumor drugs when they localize in low oxygen regions of the tumor [78], and tumor encapsulation [59]. Tumor encapsulation refers to the process by which a dense collagenous rim forms around a tumor, keeping it localized and preventing it from invading the surrounding tissue. Using a three-phase model, Jackson and Byrne showed that the capsule was more likely to form as a result of compression of the existing extracellular matrix (caused by expansion of the tumor mass) than as a result of the immune response stimulating the deposition of new collagenous material. In a related manner, Preziosi and Tosin have, more recently, used a multiphase approach to investigate how interactions between the tumor and the extracellular matrix influence the tumor's growth and remodeling of the extracellular matrix [85, 101].

Several other authors have used continuum mechanical approaches to develop models of solid tumor growth. In [27], Chaplain and Sleeman viewed the proliferating rim of a radially-symmetric expanding multicellular spheroid (MCS) as an elastic shell, enclosing a fluid-like necrotic core. A weakness of this model is that the volume of the proliferating rim does not change. Consequently, as the tumor grows, the rim gets progressively thinner: in practice, however, when MCS are cultured *in vitro* the width of the proliferating rim evolves to a constant value and, so, the volume of the proliferating rim increases as the tumor radius increases. Jones et al. formulated a single phase mechanical model in which the usual constitutive law for linear elasticity was reformulated in terms of rates of strain and stress in order to account for the continuous (and nonuniform) cell growth and death within the tumor mass [62]. A weakness of this model is that the stress becomes unbounded (and, hence, physically unrealistic) when the tumor reaches an equilibrium configuration. Several authors have since suggested modifications that resolve this deficiency. Araujo and McElwain introduce anisotropy,

assuming that cell proliferation increases the stress in the tangential direction whereas cell death relieves stress in the radial direction [8]. By contrast, MacArthur and Please show that the introduction of viscosity into the material constitutive law relieves the excessive stresses that develop in Jones et al.'s purely elastic tumor [68], while Roose et al. decompose the tumor into a two-phase mixture [88].

Other areas that merit further investigation include extending the multiphase models to two and three spatial dimensions and investigating the impact on the tumor's growth dynamics of using different constitutive laws to describe its mechanical properties. For example, we might view the cell phase as an elastic [88] or viscoelastic material. Finally, when developing mechanical models of the type discussed in this section, it is important to verify that the constitutive laws used to close the models do not violate the laws of thermodynamics (for details, see [4, 5] and references therein).

12.1.5 Conclusions

In this chapter we have reviewed a series of increasingly complex, continuum models of avascular tumor growth. These range from one-dimensional models of radially-symmetric growth (see Section 12.1.2) to two-dimensional models that can be used to determine the stability of the radially-symmetric solutions to symmetry-breaking perturbations and, hence, to establish conditions under which it remains localized (i.e., stable) and conditions under which it becomes invasive (i.e., unstable; see Section 12.1.3). In Section 12.1.4.4 we introduced a multiphase modeling approach which extended the models of Sections 12.1.2 and 12.1.3 to allow for tumor heterogeneity. We showed how the constitutive assumptions that are used to close the model influence its structure. For example, if the tumor cell and fluid phases are assumed to be incompressible, with fixed volume fractions, then moving boundary problems of the type presented in Section 12.1.2 are recovered. Alternatively, if the two phases are treated as isotropic fluids whose pressure are related by a prescribed function of the cell volume fraction then we recover reaction-diffusion models of tumor invasion similar to those proposed in [46, 89].

As mentioned in the introduction, we have focussed our review on spatially-structured continuum models and neglected the rapidly increasing number of stochastic and cell-based models of avascular tumor growth. Indeed, several probabilistic models of avascular tumor growth that reproduce the same behavior as the PDE models have been developed and shown to exhibit good qualitative and quantitative agreement with experimental data. Models of this type that focus on individual cells and their interactions with neighboring cells use concepts ranging from Markov chain processes [55], through cellular automata [6, 36, 71] to Potts models which are based on stochastic energy minimization techniques [61, 94, 103].

When comparing discrete, cell-based and continuum models of tumor growth, an obvious advantage of cell-based models is the relative ease with which parameters to model their behavior can be estimated from measurable biological and biophysical

quantities, such as cell growth rates during the cell cycle and cell membrane deformation in response to mechanical loading. Given that tumors growing *in vitro* and *in vivo* typically contain between 10^6 and 10^{11} cells, it might be more practical to use a continuum rather than a cell-based model to simulate their development. In [22], Byrne and Drasdo developed complementary cell-based and continuum models of the growth of tumor spheroids that exhibited similar growth kinetics. By fitting the profiles for the tumor radius and pressure distribution generated by each model they estimated parameters for the continuum model from parameters in the cell-based model. In this way, they have shown how cell-based models can be used as an intermediate step to relate measurable biophysical properties of individual cells to parameters that appear in continuum models of tumor spheroids.

Other authors have used theoretical approaches more formally to relate discrete and continuum models. For example, in [40] a continuum model, comprising a mixed system of partial differential equations, is derived, in the limit of large numbers of cells, to describe the dynamics of a system of tightly adherent (visco-elastic) cells which are subject to drag due to cell-substrate adhesion. In [73], Murray and coworkers show formally that is possible to model the movement of a population of individual cells connected by overdamped elastic springs by a nonlinear diffusion equation for the cell density. In [74] the approach is extended to develop a continuum model of cell movement and proliferation in which cell proliferation depends on the subcellular dynamics of particular proteins.

An exciting, alternative approach is being developed by Kim and coworkers [65]: they propose a new type of hybrid model in which a continuum model is used in regions where the tissue density does not change markedly and use a discrete, cell-based model in regions characterized by high rates of cell proliferation. One of the key challenges associated with such models is determining how to couple the continuum and discrete regions of the tissue domain.

The wide range of mathematical approaches being used to study tumor growth, and avascular tumor growth in particular, can make it difficult to know what type of model is best suited to a particular problem and what level of detail should be included. The situation can be further exacerbated when we realize that different mathematical approaches can reproduce the same experimental results! In such cases, it may be appropriate to appeal to Occam's razor and develop a model that includes sufficient detail to address the question of interest but not so much that it becomes obscured in detail. In practice, close collaboration between theoreticians and biomedical researchers is vital to getting this balance right, because the models are only ever as good as the assumptions used to construct them and the data with which they are validated. Indeed, in many respects the form of the initial model is less important than starting the dialogue between experimentalists and modelers because the model will almost certainly be wrong. In the same way that a new experimental protocol requires testing and optimization before data collection can begin, mathematical models require refinement before they can be used to address real problems.

To date, most of the mathematical modeling that has been carried out has been retrospective, being developed in response to a set of experimental data or to test a biological hypothesis. As theoreticians become more involved in experimental design the models that they develop should better represent the experimental data, and vice versa. Additionally, the quality and practical use of the mathematical models should also increase, contributing ultimately to improved treatment and a better prognosis for cancer patients worldwide.

Bibliography

[1] J. A. Adam, A simplified mathematical model of tumour growth, *Math. Biosci.* **81** (1986), 229–242.

[2] J. A. Adam, A mathematical model of tumour growth. II Effects of geometry and spatial uniformity on stability, *Math. Biosci.* **86** (1987), 183–211.

[3] J. A. Adam, N. Bellomo, *A survey of models for tumour immune system dynamics,* Birkhäuser Press, 1997.

[4] D. Ambrosi, F. Mollica, On the mechanics of a growing tumour, *Intl. J. Eng. Sci.* **40** (2002), 1297–1316.

[5] D. Ambrosi, L. Preziosi, On the closure of mass balance models for tumor growth, *Math. Models Methods Appl. Sci.* **12**, (2002), 737–754.

[6] A. R. Anderson, A hybrid mathematical model of solid tumour invasion: the importance of cell adhesion, *Math. Med. Biol.* **22** (2005), 163–186.

[7] A. R. A. Anderson, A. M. Weaver, P. T. Cummings, V. Quaranta, Tumour morphology and phenotypic evolution driven by selective pressure from the microenvironment, *Cell* **127**(5) (2006), 905–915.

[8] R. P. Araujo, D. L. S. McElwain, A history of the study of solid tumor growth: the contribution of mathematical modelling, *Bull. Math. Biol.* **66** (2004), 1039–1091.

[9] C. J. W. Breward, H. M. Byrne, C. E. Lewis, A multiphase model describing vascular tumour growth, *J. Math. Biol.* **65** (2003), 609–640.

[10] C. J. W. Breward, H. M. Byrne, C. E. Lewis, The role of cell-cell interactions in a two-phase of solid tumor growth, *J. Math. Biol.* **45** (2002), 125–152.

[11] A. C. Burton, Rate of growth of solid tumours as a problem of diffusion, *Growth* **30** (1966), 157–176.

[12] H. M. Byrne, The importance of intercellular adhesion in the development of carcinomas, *IMA J. Math. Appl. Med. Biol.* **14** (1997), 305–323.

[13] H. M. Byrne, A weakly nonlinear analysis of a model of avascular solid tumour growth, *J. Math. Biol.* **33** (1999) 59–89.

[14] H. M. Byrne, A weakly nonlinear analysis of a model of avascular solid tumour growth, *J. Math. Biol.* **33** (1999), 59–89.

Note 57: AU: [3] Publishers location is missing.

Note 58: References [13] and [14] are the same

Note 59: references [15] and [16] are the same

[15] H. M. Byrne, Mathematical modelling of solid tumour growth: from avascular to vascular, via angiogenesis, in: *IAS/Park City Mathematics Series*, Volume 14 (Editors: M. A. Lewis, M. A. J. Chaplain, J. P. Keener and P. K. Maini). American Mathematical Society, 2009.

[16] H. M. Byrne, Mathematical modelling of solid tumour growth: from avascular to vascular, via angiogenesis, in: *IAS/Park City Mathematics Series*, Volume 14 (Editors: M. A. Lewis, M. A. J. Chaplain, J. P. Keener and P. K. Maini). American Mathematical Society, 2009.

[17] H. M. Byrne, Dissecting cancer through mathematics: from the cell to the animal model, *Nature Reviews Cancer.* **10(3)** (2010), 221–230.

[18] H. M. Byrne, M. A. J. Chaplain, Growth of non-necrotic tumours in the presence and absence of inhibitors, *Math. Biosci.* **130** (1995), 151–181.

[19] H. M. Byrne, M. A. J. Chaplain, Growth of necrotic tumours in the presence and absence of inhibitors, *Math. Biosci.* **131** (1995), 187–216.

[20] H. M. Byrne, M. A. J. Chaplain, Free boundary value problem associated with the growth and development of multicellular spheroids, *Eur. J. Appl. Math.* **8** (1997), 639–658.

[21] H. M. Byrne, M. A. J. Chaplain, Necrosis and apoptosis: Distinct cell loss mechanisms in a mathematical model of solid tumour growth, *J. Theor. Med.* **1** (1998), 223–236.

[22] H. Byrne, D. Drasdo, Individual-based and continuum models of growing cell populations: a comparison, *J. Math. Biol.* **58** (2009), 657–687.

[23] H. M. Byrne, J. R. King, D. L. S. McElwain, L. Preziosi, A two-phase model of solid tumor growth, *Appl. Math. Lett.* **16** (2003), 567–573.

[24] H. M. Byrne, P. C. Matthews, Asymmetric growth of avascular tumours: exploiting symmetries, *IMA J. Math. Appl. Med. Biol.* **19** (2002), 1–29.

[25] H. M. Byrne, L. Preziosi, Modelling solid tumor growth using the theory of mixtures, *IMA J. Math. Appl. Med. Biol.* **20** (2003), 341–366.

[26] M. A. J. Chaplain, M. Ganesh, I. Graham, Spatio-temporal pattern formation on spherical surfaces: numerical simulation and application to solid tumour growth, *J. Math. Biol.* **42** (2001), 387–423.

[27] M. A. J. Chaplain, B. D. Sleeman, Modelling the growth of solid tumours and incorporating a method for their classification using nonlinear elasticity theory, *J. Math. Biol.* **31** (1993), 431–473.

[28] C. Y. Chen, H. M. Byrne, J. R. King, The influence of growth-induced stress from the surrounding medium on the development of multicell spheroids, *J. Math. Biol.* **43** (2001), 191–220.

[29] X. Chen, A. Friedman, A free boundary problem for elliptic-hyperbolic system: an application to tumour growth, *SIAM J. Math. Anal.* **35** (2003), 974–986.

[30] J. Crank, *Free and Moving Boundary Problems*, Clarendon Press, Oxford, 1984.

[31] V. Cristini, J. Lowengrub, Q. Nie, Nonlinear simulation of tumour growth, *J. Math. Biol.* **46** (2003), 191–224.

[32] S. B. Cui, A. Friedman, Analysis of a mathematical model of the effect of inhibitors on the growth of tumours, *Math. Biosci.* **164** (2000), 103–137.

[33] E. De Angelis, L. Preziosi, Advection-diffusion models for solid tumour evolution *in vivo* and related free boundary problems, *Math. Models Methods App. Sci.* **10** (2000), 379–407.

[34] D. Drasdo, S. Hoehme, M. Block, On the role of physics in the growth and pattern formation of multi-cellular systems: what can we learn from individual-cell based models?, *J. Stat. Phys.* **128** (2007), 287–345.

[35] D. A. Drew, L. A. Segel, Averaged equations for two-phase flows, *Stud. Appl. Math.* **50** (1971), 205–231.

[36] W. Duchting, Spatial structure of tumour growth: a simulation study, *IEEE Transactions on Systems, Man and Cybernetics* **10(6)** (1980), 292–296.

[37] H. Enderling, M. A. J. Chaplain, A. R. A. Anderson, J. S. Vaidya, A mathematical model of breast cancer development, local treatment and recurrence, *J. Theor. Biol.* **246(2)** (2007), 245–259.

[38] J. Folkman, M. Hochberg, Self-regulation of growth in three-dimensions, *J. Exp. Med.* **138** (1973), 745–753.

[39] A. C. Fowler, *Mathematical models in the applied sciences,* C. U. P., (1997).

[40] J. A. Fozard, H. M. Byrne, O. E. Jensen, J. R. King, Continuum approximations of individual-based models for multicellular systems, *Math. Med. Biol.* **27(1)** (2010), 39–74.

[41] S. J. Franks, H. M. Byrne, J. R. King, C. E. Lewis, Modelling the growth of ductal carcinoma in situ, *J. Math. Biol.* **47** (2003), 424–452.

[42] S. J. Franks, H. M. Byrne, H. S. Mudhar, J. C. E. Underwood, C.E. Lewis, Mathematical modelling of comedo ductal carcinoma in situ of the breast, *Math. Med. Biol.* **20** (2003), 277–308.

[43] S. J. Franks, H. M. Byrne, J. C. E. Underwood, C. E. Lewis, Biological inferences from a mathematical model of comedo duct carcinoma in situ of the breast, *J. theor. Biol.* **232** (2005), 523–543.

[44] A. Friedman, Mathematical analysis and challenges arising from models of tumour growth, *Math. Mod. Meth. Appl. Sci.* **17** (2007), 1751–1772.

[45] A. Friedman, F. Reitich, Analysis of a mathematical model for the growth of tumours, *J. Math. Biol.* **38** (1999), 262–284.

[46] R. A. Gatenby, E. T. Gawlinski, A reaction-diffusion model of cancer invasion, *Cancer Res.* **56** (1996), 5745–5753.

[47] R. A. Gatenby, E. T. Gawlinski, The glycolytic phenotype in carcinogenesis and tumor invasion: insights through mathematical models, *Cancer Res.* **63** (2003), 3847–3854.

[48] R. A. Gatenby, P. K. Maini, Mathematical oncology: Cancer summed up, *Nature* **421** (2003), 321.

Note 60: AU: [39] Publishers location is missing.

[49] H. P. Greenspan, Models for the growth of a solid tumour by diffusion, *Stud. Appl. Math.* **52** (1972), 317–340.

[50] H. P Greenspan, On the growth and stability of cell cultures and solid tumours, *J. Theor. Biol.* **56** (1976), 229–242.

[51] K. Groebe, W. Mueller-Klieser, Distributions of oxygen, nutrient and metabolic waste concentration in multicellular spheroids and their dependence on spheroid parameters, *Eur. Biophys. J.* **19** (1991), 169–181.

[52] K. Groebe, W. Mueller-Klieser, On the relation between size of necrosis and diameter of tumour spheroids, *Int. J. Radiat. Oncol.* **34** (1996), 395–401.

[53] D. Hanahan, R. A. Weinberg, The hallmarks of cancer, *Cell* **100** (2000), 57–70.

[54] D. Hanahan, R. A. Weinberg, Hallmarks of cancer: the next generation, *Cell* **144** (2011), 646–674.

[55] L. G. Hanin, A stochastic model of tumour response to fractionated radiation: limit theorems and rate of convergence, *Math. Biosci.* **191(1)** (2004), 1–17.

[56] G. Helmlinger, P. A. Netti, H. C. Lichtenbeld, R. J. Melder, R. K. Jain, Solid stress inhibits the growth of multicellular tumour spheroids, *Nature Biotech.* **15** (1997), 778–783.

[57] M. E. Hubbard, H. M. Byrne, Multiphase modelling of vascular tumour growth in two spatial dimensions, *J. Math. Biol.* (2012), (under revision).

[58] T. L. Jackson, Intracellular accumulation and mechanism of action of doxorubicin in a spatio-temporal tumour model, *J. Theor. Biol.* **220(2)** (2003), 201–213.

[59] T. L. Jackson, H. M. Byrne, A mechanical model of tumor encapsulation and transcapsular spread, *Math. Biosci.* **180** (2002), 307–328.

[60] T. L. Jackson, S. R. Lubkin, J. D. Murray, Theoretical analysis of conjugate localization in two-step cancer chemotherapy, *J. Math. Biol.* **39** (1999), 353–376.

[61] Y. Jiang, J. Pjesivan-Grbovic, C. Cantrell, J. P. Freyer, A multiscale model for avascular tumour growth, *Biophys. J.* **89** (2005), 3884–3894.

[62] A. S. Jones, H. M. Byrne, J. W. Dold, J. Gibson, A mathematical model of the stress induced during solid tumour growth, *J. Math. Biol.* **40** (2000), 473–499.

[63] C. E. Kelly, R. D. Leek, H. M. Byrne, S. M. Cox, A. L. Harris, C. E. Lewis, Modelling macrophage infiltration into avascular tumours, *J. Theor. Med.* **4** (2002), 21–38.

[64] J. F. R. Kerr, Shrinkage necrosis: a distinct mode of cell death, *J. Path.* **105** (1971), 13–20.

[65] Y. Kim, M. A. Stolarska, H. G. Othmer, A hybrid model for tumour spheroid growth *in vitro* I: theoretical development and early results, *Math. Model. Meth. Appl. Sci.* **17** (2007), S1773–S1798.

[66] K. A. Landman, C. P. Please, Tumour dynamics and necrosis: Surface tension and stability, *IMA. J. Math. Appl. Med.* **18** (2001), 131–158.

[67] C.-Y. Li, S. Shan, Q. Huang, R. D. Braun, J. Lanzen, K. Hu, L. Lin, M. W. Dewhirst, Initial stages of tumour cell-induced angiogenesis: evaluation via skin window-chambers in rodent models, *J Natl Cancer Inst* **92(2)** (2000), 143–137.

[68] B. D. MacArthur, C. P. Please, Residual stress generation and necrosis formation in multicell tumour spheroids, *J. Math. Biol.* **49** (2004), 537–552.

[69] N. Mantzaris, S. Webb, H. G. Othmer, Mathematical modelling of tumour-induced angiogenesis, *J. Math. Biol.* **95** (2004), 111–187.

[70] D. L. S. McElwain, L. E. Morris, Apoptosis as a volume loss mechanism in mathematical models of solid tumour growth, *Math. Biosci.* **39** (1978), 147–157.

[71] J. Moreira, A. Deutsch, Cellular automaton models of tumour development: a critical review, *Adv. Complex Systems* **5** (2002), 247–267.

[72] V. C. Mow, S. C. Kuei, W. M. Lai, C. G. Armstrong, Biphasic creep and stress relaxation of articular cartilage in compression: theory and experiments, *J. Biomech. Eng.* **102(1)** (1980), 73–84.

[73] P. J. Murray, C. M. Edwards, M. J, Tindall, P. K. Maini, From a discrete to a continuum model of cell dynamics in one dimension, *Phys. Rev. E* **80** (2009), 031912.

[74] P. J. Murray, J.-W. Kang, G. R. Mirams, S.-Y. Shin, H. M. Byrne, P. K. Maini, K.-H. Cho, Modelling spatially regulated β-catenin dynamics and invasion in intestinal crypts, *Biophys. J.* **99(3)** (2010), 716–725.

[75] R. D. O'Dea, J. M. Osborne, A. J. El-Haj, H. M. Byrne, S. L. Waters, The interplay between scaffold degradation, tissue growth and cell behaviour in engineered tissue constructs, *J. Math. Biol* (2012), (submitted).

[76] R. D. O'Dea, S. L. Waters, H. M. Byrne, A multiphase model for tissue construct growth in a perfusion bioreactor, *Math. Med. Biol.* **27(2)** (2010), 95–127.

[77] J. M. Osborne, R. D. O'Dea, J. P. Whiteley, H. M. Byrne, S. L. Waters, The influence of bioreactor geometry and the mechanical environment on engineered tissues, *J. Biomech. Eng.* **132** (2010), 051006.

[78] M. R. Owen, H. M. Byrne, C. E. Lewis, Mathematical modelling of the use of macrophages as vehicles for drug delivery to hypoxic tumour sites, *J. Theor. Biol.* **226** (2004), 377–391.

[79] H. Perfahl, M. R. Owen, T. Alarcon, A. Lapin, P. K. Maini, M. Reuss, H. M. Byrne, 3D hybrid multiscale modelling of vascular tumour growth, *PLoS One* **6(4)** (2011), e14790.

[80] A. J. Perumpanani, H. M. Byrne, Extracellular matrix concentration exerts selective pressure on invasive cells, *Eur. J. Cancer* **35** (1999), 1274–1280.

[81] G. J. Pettet, C. P. Please, M. J. Tindall, D. L. S. McElwain, The migration of cells in multicell tumour spheroids, *Bull. Math. Biol.* **63** (2001), 231–257.

[82] C. P. Please, G. J. Pettet, D. L. S. McElwain, A new approach to modelling the formation of necrotic regions in tumours, *Appl. Math. Letters* **11** (1998), 89–94.

[83] J. B. Plotkin, M. A. Nowak, The different effects of apoptosis and DNA repair on tumorigenesis, *J. theor. Biol.* **214** (2002), 453–467.

Note 61: AU: [84] Publishers location is missing.

[84] L. Preziosi, *Cancer modelling and simulation*, Chapman and Hall/CRC, 2003.

[85] L. Preziosi, A. Tosin, Multiphase modelling of tumour growth and extracellular matric interaction: mathematical tools and applications, *J. Math. Biol.* **58** (2009), 625–656.

[86] V. Quaranta, K. A. Rejniak, P. Gerlee, A. R. Anderson, Invasion emerges from cancer cell adaptation to competitive microenvironments: quantitative predictions from multiscale mathematical models, *Semin. Cancer Biol.* **18** (2008), 338–348.

[87] T. Roose, S. J. Chapman, P. K. Maini, Mathematical models of avascular tumour growth: a review, *SIAM Review* **49** (2006), 179–208.

[88] T. Roose, P. A. Netti, L. L. Munn, Y. Boucher, R. K. Jain, Solid stress generated by spheroid growth estimated using a linear poroelasticity model, *Microvasc. Res.* **66** (2003), 204–212.

[89] J. A. Sherratt, Cellular growth and travelling waves of cancer, *SIAM Appl. Math.* **53** (1993), 1713–1730.

[90] R. M. Shymko, L. Glass, Cellular and geometric control of tissue growth and mitotic instability, *J. Theor. Biol.* **63** (1976), 355–374.

[91] K. Smallbone, D. J. Gavaghan, R. A. Gatenby, P. K. Maini, The role of acidity in solid tumour growth and invasion, *J. Theor. Biol.* **235** (2005), 476–484.

[92] S. L. Spencer, R. A. Gerety, K. J. Pienta and S. Forrest, Modelling somatic evolution in tumorigenesis, *PLoS Comp. Biol.* **2** (2006), e108.

[93] W. G. Stetler-Stevenson, S. Aznavoorian, L. A. Liotta, Tumour cell interactions with the extracellular matrix during invasion and metastasis, *Ann. Rev. Cell. Biol.* **9** (1993), 541–573.

[94] E. L. Stott, N. F. Britton, J. A. Glazier, M. Zajac, Stochastic simulation of benign avascular tumour growth using the Potts model, *Math. Comp. Mod.* **30** (1999), 183–198.

[95] R. M. Sutherland, R. E. Durand, Growth and cellular characteristics of multicell spheroids, *Recent Results in Cancer Research* **95** (1984), 24–49.

[96] K. R. Swanson, E. C. Alvord, J. D. Murray, A quantitative model for differential motility of gliomas in grey and white matter, *Cell. Prolif.* **33** (2000), 317–329.

[97] K. R. Swanson, E. C. Alvord, J. D. Murray, Quantifying efficacy of chemotherapy of brain tumors with homogeneous and heterogeneous drug delivery, *Acta Biotheoretica* **50** (2002), 223–237.

[98] K. R. Swanson, C. Bridge, J. D. Murray, E. C. Alvord, Virtual and real brain tumors: using mathematical modeling to quantify glioma growth and invasion, *J. Neur. Sci.* **216** (2003), 1–10.

[99] K. R. Swanson, R. C. Rockne, J. Claridge, M. A. Chaplain, E. C. Alvord Jr., A. R. Anderson, Quantifying the role of angiogenesis in malignant progression of gliomas: In silico modeling integrates imaging and histology, *Cancer Res.* **71** (2011), 7366.

[100] K. E. Thompson, H. M. Byrne, Modelling the internalisation of labelled cells in tumour spheroids, *Bull. Math. Biol.* **61** (1999), 601–623.

[101] A. Tosin, L. Preziosi, Multiphase modelling of tumour growth with matrix remodelling and fibrosis, *Math. Comp. Modelling* **52** (2010), 969–976.

[102] P. Tracqui, From passive diffusion to active cellular migration in mathematical models of tumour invasion, *Acta Biotheoretica* **43** (1995), 443–464.

[103] S. Turner, J. A. Sherratt, Intercellular adhesion and cancer invasion: a discrete simulation using the extended Potts model, *J. Theor. Biol.* **216** (2002), 85–100.

[104] I. M. M. van Leeuwen, G. R. Mirams, A. Walter, P. Murray, J. Osborne, S. Varma, S. J. Young, J. Cooper, B. Doyle, J. Pitt-Francis, L. Momtahan, P. Pathmanathan, J. P. Whiteley, S. J. Chapman, D. J. Gavaghan, O. E. Jensen, J. R. King, P. K. Maini, S. L. Waters, H. M. Byrne, An integrative computational model for intestinal tissue renewal, *Cell Prolif.* **42** (2009), 617–636.

[105] J. P. Ward, J. R. King, Mathematical modelling of avascular-tumour growth, *IMA. J. Math. Appl. Med.* **14** (1997), 39–69.

[106] J. P. Ward, J. R. King, Mathematical modelling of avascular-tumour growth II: Modelling growth saturation, *IMA. J. Math. Appl. Med.* **15** (1998), 1–42.

[107] J. P. Ward, J. R. King, Mathematical modelling of the effects of mitotic inhibitors on avascular tumor growth, *J. Theor. Med.*, **1** (1999), 171–211.

[108] S. D. Webb, J. A. Sherratt, G. Fish, Alterations in proteolytic activity at low pH and its association with invasion: a theoretical model, *Clin. Exptl. Metastasis* **17(5)** (1999), 397–407.

[109] L. M. Wein, J. T. Wu, D. H. Kirn, Validation and analysis of a mathematical model of a replication-competent oncolytic virus for cancer treatment: implications for virus design and therapy, *Cancer Res.* **15** (2003), 1317–1324.

Author Information

Helen M. Byrne, Oxford Centre for Collaborative and Applied Mathematics, Mathematical Institute, Oxford, UK
E-mail: `helen.byrne@maths.ox.ac.uk`

RECENT REPORTS

12/73	Bounds on the solution of a Cauchy-type problem involving a weighted sequential fractional derivative	Furati
12/74	Static and dynamic stability results for a class of three-dimensional configurations of Kirchhoff elastic rods	Majumdar Goriely
12/75	Error estimation and adaptivity for incompressible, nonlinear (hyper)elasticity	Whiteley Tavener
12/76	A note on heat and mass transfer from a sphere in Stokes flow at low Péclet number	Bell Byrne Whiteley Waters
12/77	Effect of disjoining pressure in a thin film equation with non-uniform forcing	Moulton Lega
12/78	A Review of Mathematical Models for the Formation of Vascular Networks	Scianna Bell Preziosi
12/79	Fast and Accurate Computation of Gauss-Legendre and Gauss-Jacobi Quadrature Nodes and Weights	Hale Townsend
12/80	On the spectral distribution of kernel matrices related to radial basis functions	Wathen Zhu
12/81	Inner product computation for sparse iterative solvers on distributed supercomputer	Zhu Gu Liu
12/82	A new pathway for the re-equilibration of micellar surfactant solutions	Griffiths Breward Colegate Dellar Howell Bain
12/83	Object-Oriented Paradigms for Modelling Vascular Tumour Growth: a Case Study	Connor Cooper Byrne Maini McKeever
12/84	Chaste: an open source C++ library for computational physiology and biology	Mirams Arthurs Bernabeu Bordas Cooper Corrias Davit Dunn Fletcher Harvey Marsh Osborne Pathmanathan

12/86	Boolean modelling reveals new regulatory connections between transcription factors orchestrating the development of the ventral spinal cord	Lovrics Gao Juhász Bock Byrne Dinnyés Kovács
12/87	Asymptotic solutions of glass temperature profiles during steady optical fibre drawing	Taroni Breward Cummings Griffiths
12/88	The kinetics of surfactant desorption at the airsolution interface	Morgan Breward Griffiths Howell Penfold Thomas Tucker Petkov Webster
12/89	An experimental and theoretical investigation of particlewall impacts in a T-junction	Vigolo Griffiths Radl Stone
12/90	Transitions through Critical Temperatures in Nematic Liquid Crystals	Majumdar Ockendon Howell Surovyatkina
12/91	Biaxial defect cores in nematic equilibria: an asymptotic result	Majumdar Pisante Henao
12/92	The Three Sphere Swimmer in a Nonlinear Viscoelastic Medium	Curtis Gaffney
12/93	Diffusion of multiple species with excluded-volume effects	Bruna Chapman
12/94	The Mechanics of a Chain or Ring of Spherical Magnets	Hall Vella Goriely
12/95	On-Lattice Agent-based Simulation of Populations of Cells within the Open-Source Chaste Framework	Figueredo Joshi Osborne Byrne Owen

Copies of these, and any other OCCAM reports can be obtained from:

Oxford Centre for Collaborative Applied Mathematics
Mathematical Institute
24 - 29 St Giles'
Oxford
OX1 3LB
England
www.maths.ox.ac.uk/occam